NOAA Technical Report ERL 400–ARL 6

NOAA Air Resources Laboratories

Stratospheric Lidar Project 1976 Results

Ronald W. Fegley

September 1978

U.S. DEPARTMENT OF COMMERCE
National Oceanic and Atmospheric Administration
Environmental Research Laboratories

NOAA Technical Report ERL 400–ARL 6

NOAA Air Resources Laboratories

Stratospheric Lidar Project 1976 Results

Ronald W. Fegley

Air Resources Laboratories/GMCC
Boulder, Colorado

September 1978

U.S. DEPARTMENT OF COMMERCE
Juanita Kreps, Secretary

National Oceanic and Atmospheric Administration
Richard A. Frank, Administrator

Environmental Research Laboratories
Wilmot Hess, Director

NOTICE

Mention of a commercial company or product does not constitute an endorsement by NOAA Environmental Research Laboratories. Use for publicity or advertising purposes of information from this publication concerning proprietary products or the tests of such products is not authorized.

CONTENTS

NOAA AIR RESOURCES LABORATORIES STRATOSPHERIC LIDAR PROJECT 1976 RESULTS

Ronald W. Fegley

ABSTRACT. The NOAA Air Resources Laboratories have conducted a stratospheric measurement project since 1973 at the Mauna Loa Observatory in Hawaii (19.5° N, 155.6° W). Lidar soundings of stratospheric aerosols are taken biweekly, using a ruby laser with a wavelength of 694.3 nm. This report covers 1976. Nine profiles of the non-Rayleigh backscatter coefficient are plotted and tabulated throughout the lower stratosphere from 16 to 25 km. These aerosols, which are of climatic importance, displayed a decreasing trend during 1976 as the stratosphere recovered from the October 1974 eruption of Fuego volcano in Guatemala (14.5° N, 91° W).

1. INTRODUCTION

There is strong support within the meteorological community for the idea that substantial portions of the short-term fluctuations (one to several years) in global surface temperature may be caused by volcanically induced changes in the stratospheric aerosol burden (Mitchell, 1975).

There is theoretical evidence for the concept that increases in stratospheric aerosol will produce cooling at the earth's surface, assuming reasonable atmospheric parameters (Pollack et al., 1976; Coakley and Grams, 1976; Harshvardhan and Cess, 1976). Although the predictions vary depending upon the model, cooling of several tenths of a degree Celsius is typical for a moderate eruption such as that of Gunung Agung in Indonesia in 1963. Mitchell (1975) states that the typical waiting period for such an eruption is approximately 20 years.

There is some experimental support for these predictions. Mitchell (1970) discusses an analysis in which he estimated a cooling anomaly of approximately 0.1 °C for five years after a "typical" eruption. The temperature record he used extended from 1870 to 1960.

More recently, Oliver (1976) compared volcanic dust data with Northern Hemisphere temperature records and showed a fair correlation. Surface cooling anomalies were reproduced for several major volcanic events since 1881, and the relatively warm period from 1920 to 1940 is seen to be plausibly related to the scarcity of major volcanic eruptions. Hoyt (1978) has enhanced Oliver's analysis by finding evidence for volcanic injections in 1928 and 1932, which explains two temperature dips at those times in the record.

Mass and Schneider (1977) used the method of statistical compositing to study the relationship between surface temperature records and stratospheric dust concentrations. They detected a definite surface cooling following major volcanic injections.

The stratospheric aerosol layer normally fluctuates in intensity, particularly after major volcanic injections of sulfur-bearing gasses and debris (Cadle and Grams, 1975). Major penetrations of the stratosphere are produced by large eruptions, such as those of Indonesia's Krakatoa and Agung, and the residence time for these aerosols can easily be 1 to 2 years. More frequently, less intense eruptions can enhance the layer in the lower stratosphere, producing radiative perturbations of a few months' duration (Fegley and Ellis, 1975b).

In order to complete our understanding of this climatic phenomenon, it is necessary to acquire observational data on the amount, geographical distribution, and radiative properties of these volcanic clouds as they evolve. A common lament in the aforementioned papers concerns the dearth of observational data for the major eruptions during the period of reliable temperature data. It is necessary to speculate to a large degree about the dust cloud parameters for each event. With such poor data, the calculated temperature anomalies are subject to large error, and comparison with measured temperatures is difficult.

In order to be ready for future major eruptions, NOAA has planned a network of laser radar (lidar) systems to be located at its Geophysical Monitoring for Climatic Change baseline stations situated at various latitudes (NOAA, 1977). Lidar is a practical way to monitor the stratospheric aerosol layer and has shown good agreement with other sampling methods (Northam et al., 1974; Russell et al., 1976).

During 1972, a ruby Lidar system (Fegley et al., 1978) was installed at the NOAA Mauna Loa Observatory at 3.4 km altitude on the island of Hawaii (19°32' N, 155°35' W). A fortnightly observation schedule was established in April 1973, and has continued to the present. The data are now archived in Boulder, Colorado, and will be published periodically as NOAA/ERL Data Reports. Brief reports have appeared recently (NOAA, 1976; Fegley and Ellis, 1975a and b).

Lidar has an advantage over surface-based radiation measurements in the monitoring of stratospheric aerosol concentrations. With lidar, one can unambiguously state that the aerosols are in the stratosphere, whereas, with radiometers, the perceived radiation decreases may be due to low-altitude pollution, tropospheric aerosols, sub-visible cirrus, or other factors.

2. LIDAR SYSTEM DESCRIPTION

Briefly, the lidar system consists of the components shown in Fig. 1. The ruby laser fires a pulse of light into the atmosphere. This pulse typically has an energy of 1 joule, a duration of 30 nsec, and a peak power of 30 megawatts. The wavelength is 694.3 nm. The pulse is triggered by a signal from the master timing control box which is sent to the laser power supply. A photodiode at the back of the laser generates a pulse at the actual time of firing. This pulse triggers the transient digitizer which then begins to acquire data from the receiver system.

The signal backscattered from the atmosphere is collected by a Schmidt-Cassegrain telescope with an aperture of 40 cm diameter. The exiting bundle of rays is collimated with a positive lens. This light then passes through an interference filter having a 1 nm passband. The light is detected with an RCA model 7265 photomultiplier tube.

The resulting electrical signal is filtered through a sharp low-pass filter having a cutoff frequency of 4 MHz. It is then digitized and stored in the transient digitizer. Upon command, a NOVA minicomputer reads out the stored data and processes them. The raw data are then punched onto paper tape for archiving purposes and future analysis. The results of the analysis are printed on a teletype for archiving in Boulder. These results are also archived on magnetic tape at the National Climatological Center in Asheville, North Carolina.

For a complete system description, the reader is referred to Fegley et al. (1978).

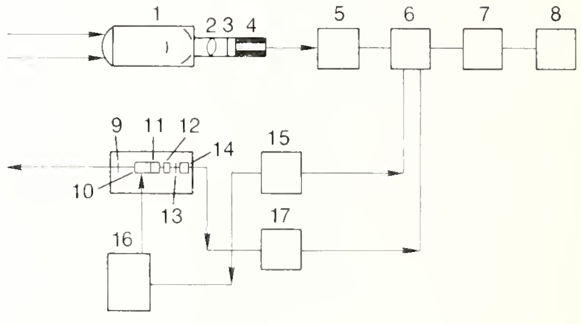

Figure 1. Hardware arrangement for Mauna Loa lidar. (1) 40 cm diameter Schmidt Cassegrain telescope. (2) Collimating lens. (3) 1 nm bandpass interference filter. (4) RCA 7265 photomultiplier tube. (5) Low pass filter, 24 dB/octave, cutoff at 4 MHz. (6) Biomation model 8100 transient digitizer. (7) NOVA model 2–10 minicomputer. (8) Teletype terminal-data output. (9) Low reflectance laser output mirror. (10) Ruby rod-flashlamp. (11) Pockels cell Q switch. (12) Brewster stack polarizer. (13) Maximum reflectance mirror. (14) Silicon photodiode laser beam detector. (15) Master timing control box. (16) Laser power supply. (17) Beam monitor integrator.

3. DATA PROCESSING

Output data voltages from the lidar photomultiplier tube (PMT) are digitized and stored by a Biomation model 8100 transient digitizer (Fig. 1). This instrument has an eight-bit word so the ultimate precision of the stored data can be no better than approximately 0.5% of the digitizer full scale. This can produce large errors at long ranges where the signal may be comparable with the uncertainty. For this reason, we normally use only the region of the return signal above about 5% of full scale. Since the dynamic range of the return signal is several orders of magnitude for a complete profile from ground level to the mid-stratosphere, it is necessary to use some form of signal compression. Our technique consists of changing the PMT voltage between series of shots.

At Mauna Loa Observatory (MLO) we find that when the PMT voltage is adjusted properly, the output voltage passes through the 95% full scale point at about 13 km msl and through the 5% level at about 23 km msl. This is a desirable situation.

In the making of lidar observations it is very difficult to absolutely calibrate the system. The usual procedure is to assume that some level of the atmosphere is aerosol- and cloud-free and that the lidar return from that level is purely Rayleigh (Barrett and Ben-Dov, 1967). When the temperature-pressure profile of the atmosphere is known, it is possible to subtract the Rayleigh backscatter from the absolute returns to derive the excess, or non-Rayleigh, backscatter as a function of altitude.

At Mauna Loa, we have almost always found the clean layer at or slightly below the tropopause, at approximately 15.5 km msl (Fernald and Schuster, 1977), so the altitude levels reported above include the calibration altitude near the tropopause, as well as the lower stratosphere, within the range of acceptable accuracy.

We also adjust the baseline of our return pulses so that a scattering ratio of 1.0 is produced at the greatest range, typically 33 km. This compensates for any baseline shift or background noise. The adjustment is very slight and has little effect at the altitude region of interest. These adjustments guarantee that there will always be at least two regions of pure Rayleigh atmosphere, one at the longest range and another at some intermediate altitude, usually near the tropopause.

The digitizer takes 2048 samples of the return signal, usually at 15 m increments of range. Our processor averages these by 20's to produce approximately 102 points along the atmospheric profile. This gives us a range resolution of 0.3 km. We usually take a series of 10 laser shots to produce a single profile, so each of our 102 final points consists of the average of 200 samples (10 shots × 20 points average per shot) of the return signal from the range of interest.

The 102 data points are then recorded on paper tape for archiving. The processor corrects the data for the $1/R^2$ range effect, the atmospheric density as a function of range (from the U.S. Standard Tropical Atmosphere), and the Rayleigh extinction along the two-way path. The result is a relative profile of backscatter which is normalized, or calibrated, as described above.

These calibrated results are then tabulated between any desired altitude limits with any desired amount of spatial averaging greater than 0.3 km.

For this report we have included the data in two formats: a graph of non-Rayleigh backscatter at 1 km altitude intervals (Fig. 2), and a tabulation of the non-Rayleigh backscatter coefficient (NRBC) at 1 km intervals (Appendix).

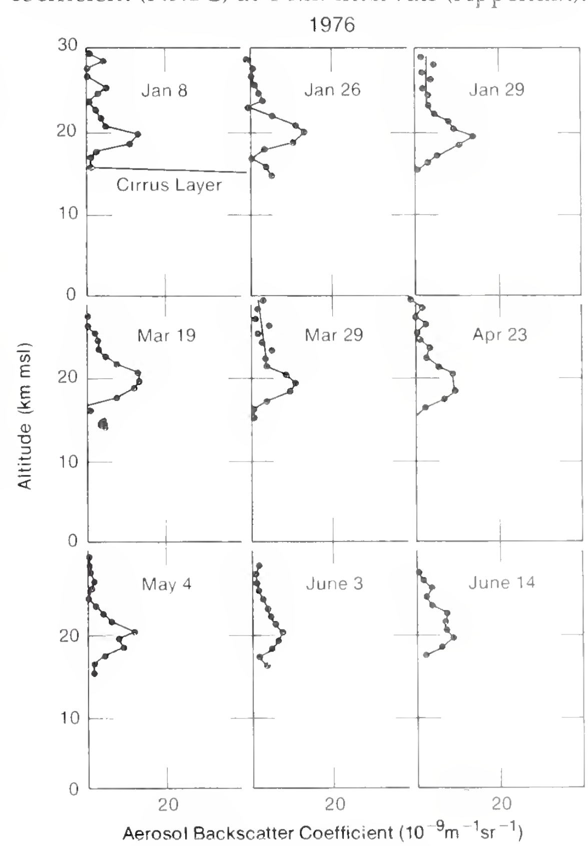

Figure 2. Non-Rayleigh backscatter coefficient as a function of altitude. Data taken at Mauna Loa Observatory.

4. PERIODS OF DATA

We attempted to make observations every other week in 1976. Excluding days of cloudy weather and periods of hardware malfunctioning, 18 data sets were taken. Nine of these were subsequently discovered to be unusable, either because of unrecognized equipment problems or operator errors. Three usable data sets were taken in January, two in March, one in April, one in May, and two in June.

During the second half of the year data-gathering was hampered by a computer breakdown, a major hardware reconfiguration, and a subtle problem with the digitizer. No data sets were taken after June. This is a common experience in field work using sophisticated instrumentation.

5. CALCULATION OF OTHER AEROSOL PARAMETERS

The lidar results are expressed in terms of the non-Rayleigh backscatter coefficient at 694.3 nm as a function of altitude. This is the physical quantity measured by the lidar. It includes an assumption that the backscatter corresponds to pure Rayleigh scattering at some level of the atmosphere where we can calibrate the system.

Some investigators may be interested in other physical parameters. One may calculate these by using an appropriate optical model or one may do simultaneous determinations of the two or more quantities of interest and thereby "calibrate" the lidar system. For example, Northam et al. (1974) compared lidar backscatter to dustsonde measurements and found an equivalence between the two. This "calibration" may be a stable value and therefore generally useful.

Investigations of the stratospheric aerosol have shown that its physical properties tend to remain fairly constant over long time periods. By and large, the composition seems to be a 75% sulfuric acid solution. The particles may be supercooled droplets or at least liquid-coated so that they are near spherical, making Mie theory calculations reasonable. These assumptions are probably less valid after volcanic injections when there may be large quantities of tephra present; however, these quickly settle out.

There seems to be considerable variation among the size distributions measured by various investigators (Cadle and Grams, 1975). However, there does seem to be a tendency for dN/d(Log r) to have a slope of −2 through the optically important region of 0.1 to 1.0 μm. Additionally, Pinnick et al. (1976) have shown that, for reasonable assumptions about the size distribution based upon their experimental data, the lidar backscatter is relatively insensitive to the exact size distribution. At least in the stratosphere, the "calibration" approach may be satisfactory over moderately long time and space intervals.

One such experiment was conducted by Northam et al. (1974) during 1972 in Laramie, Wyoming. They compared the data from a balloon-borne dustsonde (particles/cm^3) with simultaneous lidar data ($m^2/m^3\ sr^{-1}$). They found that, within the stratosphere, the lidar returns were proportional to the dustsonde data with a calibration factor of 1 particle/cm^3 corresponding to a backscatter coefficient of $7 \times 10^{-9}\ m^{-1}\ sr^{-1}$ ±14%. This measurement was made at a time when stratospheric aerosol number densities were at rather low values, so it may be representative of times well after volcanic injections at mid-latitudes.

Russell et al. (1976) have calculated conversion coefficients for lidar data based on a stratospheric optical model. They assumed that the aerosol consisted of a 75% H_2SO_4 aqueous solution with a spherical shape and a Deirmendjian Haze H size distribution. They calculated the lidar backscatter coefficient, extinction coefficient, and number and mass densities, and arrived at the following correlations:

- 1 particle/cm^3 number density is equivalent to $1.97 \times 10^{-9}\ m^{-1} sr^{-1}$.
- 0.01 km^{-1} extinction coefficient is equivalent to $1.3 \times 10^{-7}\ m^{-1} sr^{-1}$.
- 1 $\mu g\ m^{-3}$ mass density is equivalent to $3.84 \times 10^{-8}\ m^{-1} sr^{-1}$.

We plan to compare the results from the lidar observations with those from other instruments at opportune times. Such instruments might be balloon-borne particle counters (University of Wyoming), impactors (NASA, Ames), or radiometers (University of Alaska).

6. DISCUSSION OF DATA

In general, the data show a trend toward clearing of the stratospheric aerosol that has been present since the small injection by Fuego volcano (Guatemala) in late 1974 (Fegley and Ellis, 1975a). The maximum non-Rayleigh backscatter coefficient went from an average of about 12×10^{-9} to about $8 \times 10^{-9}\ m^{-1}\ sr^{-1}$ during the period of

January 8 to June 14. The vertical extent of the layer was typically between 18 and 22 km msl.

There was no obvious indication of a stratospheric enhancement as reported by Shaw (1978). He concluded that the dust from St. Augustine volcano in Alaska (59.6° N, 153.7° W), which erupted during January 1976, had increased the atmospheric extinction above Mauna Loa. Large-scale eddy processes in the midlatitude probably would have removed much of the stratospheric debris from St. Augustine before it reached Hawaii. It is more likely that the reduction in atmospheric extinction observed by Shaw was in part due to the continued stratospheric recovery from the October 1974 eruption of Fuego volcano in Guatemala.

Using the optical model of Russell et al. (1976), the particle number density at 20 km works out to about 5 particles cm^{-3} during the period. The extinction coefficient due to aerosols at 20 km is 0.0008 km^{-1}, and the mass density at 20 km is about 0.3 $\mu g\ m^{-3}$.

7. ACKNOWLEDGMENTS

The author would like to thank Howard T. Ellis for his major contribution in the development and operation of the lidar program. Earl Barrett is to be thanked for designing and building the lidar system. He has also been continuously helpful over the years as a consultant regarding problems with the hardware and data interpretation. John DeLuisi is to be thanked for many useful discussions.

8. REFERENCES

Barrett, E. W. and O. Ben-Dov (1967): Application of the lidar to air pollution measurements. *J. Appl. Meteorol.*, 6:500–515.

Cadle, R. D. and G. W. Grams (1975): Stratospheric aerosol particles and their optical properties. *Rev. Geophys. and Space Phys.* 13:475–501.

Coakley, J. A. and G. W. Grams (1976): Relative influence of visible and infrared optical properties of a stratospheric aerosol layer on the global climate. *J. Appl. Meteorol.*, 15:679–691.

Fegley, R. W., E. W. Barrett and H. T. Ellis (1978): Lidar measurements at Mauna Loa Observatory. To be included in the Mauna Loa 20th Anniversary Volume, J. Miller, ed.

Fegley, R. W. and H. T. Ellis (1975a): Lidar observations of a stratospheric dust cloud layer in the tropics. *Geophys. Res. Lett.*, 2:139–141.

Fegley, R. W. and H. T. Ellis (1975b): Optical effects of the 1974 stratospheric dust cloud. *Appl. Optics*, 14:1751–1752.

Fernald, F. G. and B. G. Schuster (1977): Wintertime 1973 airborne lidar measurements of stratospheric aerosols. *J. Geophys. Res.*, 82:433–437.

Harshvardhan and R. D. Cess (1976): Stratospheric aerosols: effect upon atmospheric temperature and global climate. *Tellus*, 28:1–9.

Hoyt, D. V. (1978): An explosive volcanic eruption in the Southern Hemisphere in 1928, unpublished manuscript.

Mass, C. and S. H. Schneider (1977): Statistical evidence on the influence of sunspots and volcanic dust on long-term temperature records. *J. Atmos. Sci.*, 34:1995–2004.

Mitchell, J. M. (1970): A preliminary evaluation of atmospheric pollution as a cause of the global temperature fluctuation of the past century. In: S. F. Singer (ed.), *Global effects of environmental pollution*. Springer-Verlag, N.Y., 139–155.

Mitchell, J. M., Jr. (1975): Note on solar variability and volcanic activity as potential sources of climatic variability. In: *The physical basis of climate and climate modelling*, GARP No. 16, World Meteorological Organization, Geneva, Switzerland.

NOAA (1976): Geophysical monitoring for climatic change — No. 4, summary report 1975. J. Watkins, ed., NOAA ERL, Boulder, Colo.

NOAA (1977): A plan for surface-based monitoring of climatically important variables, Volume 1, Project development plan, NOAA ARL, Boulder, Colo., 22–24.

Northam, G., J. Rosen, S. Melfi, T. Pepin, M. McCormick, D. Hofmann, and W. Fuller, Jr. (1974): Dustsonde and lidar measurements of stratospheric aerosols: a comparison. *Appl. Optics*, 13:2416–2421.

Oliver, R. C. (1976): On the response of hemispheric mean temperature to stratospheric dust: an empirical approach. *J. Appl. Meteorol.*, 15:933–950.

Pinnick, R. G., J. M. Rosen and D. J. Hofmann (1976): Stratospheric aerosol measurements III: optical model calculations. *J. Atmos. Sci.*, 33:304–314.

Pollack, J. B., O. B. Toon, C. Sagan, A. Summers, B. Baldwind, and W. Van Camp (1976): Volcanic explosions and climatic change: a theoretical assessment. *J. Geophys. Res.*, 81:1071–1083.

Russell, P., W. Viezee, R. Hake, Jr., and R. Collis (1976): Lidar observations of the stratospheric aerosols: California, October 1972 to March 1974. *Q. J. R. Meteorol. Soc.*, 102:675–695.

Shaw, G. E. (1978): Multi-wavelength turbidity at the Mauna Loa Observatory. Rep. no. UAG R–251, Geophysical Institute, University of Alaska, Fairbanks, Alaska.

APPENDIX
Non-Rayleigh Backscatter Coefficients at One Kilometer Intervals

	Height (km msl)	Non-Rayleigh Backscatter Coefficient	Scattering Ratio[2]
	15.5185	2.17812E − 9	1.01994
	16.5517	1.54725E − 9	1.02079
	17.4374	3.63257E − 9	1.05328
	18.4706	1.19056E − 8	1.21498
	19.5039	1.33271E − 8	1.28813
	20.5371	5.41259E − 9	1.14324
	21.5704	4.86937E − 9	1.14908
Date	22.456	3.70259E − 9	1.13338
1−8−76	23.4892	1.74153E − 9	1.07189
Time[1] (LST)	24.5225	4.20506E − 9	1.21832
1910	25.5557	7.39684E − 9	1.45354
	26.539	1.47649E − 9	1.10969
	27.4746	9.61839E − 10	1.06877
	28.5079	5.67655E − 9	1.56523
	29.5411	1.92558E − 9	1.22214
	30.4267	2.05292E − 9	1.27356
	31.46	−4.10119E − 10	0.936593
	32.4932	4.12956E − 11	1.01093
	14.4852	5.20468E − 9	1.04746
	15.5185	4.02273E − 9	1.04229
	16.5517	−2.34574E − 11	1.00067
	17.4374	2.67665E − 9	1 04061
Date	18.4706	9.89925E − 9	1.17699
1−26−76	19.5039	1.2574E − 8	1.27391
Time (LST)	20.5371	1.01268E − 8	1.26081
1956	21.5704	3.99619E − 9	1.12844
	22.456	−1.88508E − 9	0.931735
	23.4892	2.02881E − 9	1.0847
	24.5225	3.55975E − 10	1.01658
	25.5557	−6.44952E − 10	0.9601
	15.5185	−5.96948E − 10	0.994056
	16.5517	1.15921E − 9	1.01477
	17.4374	3.59201E − 9	1.05321
	18.4706	9.11083E − 9	1.16397
	19.5039	1.3287E − 8	1.28757
	20.5371	7.74529E − 9	1.1999
	21.5704	7.10108E − 9	1.22585
Date	22.456	3.51239E − 9	1.12713
1−29−76	23.4892	2.27675E − 9	1.10036
Time (LST)	24.5225	1.97026E − 9	1.10151
1920	25.5557	1.51057E − 9	1 09026
	26.589	2.82478E − 9	1.20336
	27.4746	1.37794E − 9	1.11686
	28.5079	3.32991E − 9	1.32472
	29.5411	1.03525E − 9	1.12006
	30.4267	9.73219E − 10	1 12583
	31.46	7.59112E − 10	1.11996
	32.4932	4.32588E − 10	1.08057

[1] Time is local standard time.

[2] Scattering ratio is ratio of Rayleigh plus non-Rayleigh backscatter at a given altitude to pure Rayleigh at that altitude.

	Height (km msl)	Non-Rayleigh Backscatter Coefficient	Scattering Ratio
	15.5185	8.8253E−10	1.00992
	16.5517	7.94221E−10	1.01014
	17.4374	7.59102E−9	1.11315
	18.4706	1.24425E−8	1.22231
	19.5039	1.43782E−8	1.31296
	20.5371	1.39012E−8	1.36146
	21.5704	8.70956E−9	1.27257
Date	22.456	6.564E−9	1.24156
3−19−76	23.4892	5.31443E−9	1.22958
Time (LST)	24.5225	5.21304E−9	1.26756
2012	25.5557	5.25918E−9	1.32196
	26.589	3.51546E−9	1.25292
	27.4746	4.05769E−9	1.33296
	28.5079	2.78793E−9	1.26962
	29.5411	2.83631E−9	1.32799
	30.4267	1.81954E−9	1.2375
	31.46	1.72536E−9	1.27199
	32.4932	2.84092E−10	1.04876
	15.5185	5.89274E−10	1.00677
	16.5517	6.15988E−10	1.00838
	17.4374	3.80369E−9	1.05748
	18.4706	9.6955E−9	1.17417
	19.5039	1.08491E−8	1.23241
	20.5371	9.18795E−9	1.24002
	21.5704	4.17411E−9	1.12861
Date	22.456	3.50682E−9	1.12862
3−29−76	23.4892	4.94755E−9	1.21509
Time (LST)	24.5225	3.24986E−9	1.16727
1928	25.5557	1.98569E−9	1.1178
	26.589	4.62597E−9	1.33101
	27.4746	1.59685E−9	1.13239
	28.5079	1.83325E−9	1.17865
	29.5411	3.09613E−9	1.34991
	30.4267	1.39483E−9	1.18063
	31.46	1.4354E−9	1.21859
	32.4932	1.71621E−10	1.03118
	16.5517	1.43388E−9	1.01831
	17.4374	5.51353E−9	1.08182
	18.4706	9.43443E−9	1.16803
	19.5039	8.20817E−9	1.17702
	20.5371	8.60488E−9	1.22543
	21.5704	5.51698E−9	1.1706
	22.456	2.59293E−9	1.0946
Date	23.4892	3.59777E−9	1.1534
4−23−76	24.5225	1.25269E−9	1.06081
Time (LST)	25.5557	9.48773E−10	1.05453
1957	26.589	2.81726E−9	1.20504
	27.4746	8.20387E−10	1.07083
	28.5079	2.45719E−9	1.23817
	29.5411	−9.71312E−11	0.991112
	30.4267	1.80364E−9	1.23542
	31.46	3.35624E−10	1.04347
	32.4932	2.81822E−10	1.04747

	Height (km msl)	Non-Rayleigh Backscatter Coefficient	Scattering Ratio
Date 5–4–76 Time (LST) 2026	16.5517	3.90813E−10	1.00584
	17.4374	3.8696E−9	1.05703
	18.4706	7.77939E−9	1.13774
	19.5039	6.81069E−9	1.1484
	20.5371	1.1065E−8	1.2898
	21.5704	5.37301E−9	1.16636
	22.456	3.62915E−9	1.13237
	23.4892	1.58263E−9	1.06894
	24.5225	−1.62821E−11	0.997873
	25.5557	1.33098E−9	1.08071
	26.589	1.77479E−9	1.13246
	27.4746	1.32942E−9	1.11174
	28.5079	1.35005E−9	1.13881
	29.5411	9.52485E−10	1.11119
	30.4267	9.94472E−10	1.13449
	31.46	1.02149E−9	1.16625
	32.4932	2.96782E−10	1.04036
Date 6–3–76 Time (LST) 1951	16.5517	1.47016E−9	1.01813
	17.4374	3.64314E−10	1.00499
	18.4706	3.28777E−9	1.05952
	19.5039.	5.49435E−9	1.11915
	20.5371	6.84019E−9	1.17713
	21.5704	4.96174E−9	1.15665
	22.456	3.65962E−9	1.13494
	23.4892	3.07252E−9	1.13488
	24.5225	2.14382E−9	1.11065
	25.5557	1.0886E−9	1.06908
	26.589	1.27414E−9	1.09276
	27.4746	9.80358E−10	1.08245
	28.5079	1.27995E−9	1.12409
	29.5411	8.98079E−11	1.00686
	30.4267	5.22561E−10	1.07309
	31.46	2.72329E−11	1.00126
	32.4932	−1.71505E−9	0.690801
Date 6–14–76 Time (LST) 2020	16.5517	2.01093E−10	1.00262
	17.4374	2.95116E−9	1.04531
	18.4706	6.40149E−9	1.11498
	19.5039	9.3842E−9	1.20361
	20.5371	7.58519E−9	1.19709
	21.5704	7.8313E−9	1.24411
	22.456	8.3863E−9	1.30062
	23.4892	4.71411E−9	1.21233
	24.5225	2.90972E−9	1.14301
	25.5557	4.4478E−9	1.26992
	26.589	1.96096E−9	1.13845
	27.4746	1.11425E−9	1.09255
	28.5079	7.15191E−10	1.07605
	29.5411	2.26544E−9	1.25499
	30.4267	1.78925E−9	1.24025
	31.46	2.001E−9	1.2922
	32.4932	1.89782E−10	1.03938

☆ U.S. GOVERNMENT PRINTING OFFICE: 1978-0- 677-072/1208

Environmental Research LABORATORIES

The mission of the Environmental Research Laboratories (ERL) is to conduct an integrated program of fundamental research, related technology development, and services to improve understanding and prediction of the geophysical environment comprising the oceans and inland waters, the lower and upper atmosphere, the space environment, and the Earth. The following participate in the ERL missions:

MESA *Marine EcoSystems Analysis Program.* Plans, directs, and coordinates the regional projects of NOAA and other federal agencies to assess the effect of ocean dumping, municipal and industrial waste discharge, deep ocean mining, and similar activities on marine ecosystems.

OCSEA *Outer Continental Shelf Environmental Assessment Program Office.* Plans and directs research studies supporting the assessment of the primary environmental impact of energy development along the outer continental shelf of Alaska; coordinates related research activities of federal, state, and private institutions.

W/M *Weather Modification Program Office.* Plans and coordinates ERL weather modification projects for precipitation enhancement and severe storms mitigation.

NHEML *National Hurricane and Experimental Meteorology Laboratory.* Develops techniques for more effective understanding and forecasting of tropical weather. Research areas include: hurricanes and tropical cumulus systems; experimental methods for their beneficial modification.

RFC *Research Facilities Center.* Provides aircraft and related instrumentation for environmental research programs. Maintains liaison with user and provides required operations or measurement tools, logged data, and related information for airborne or selected surface research programs.

AOML *Atlantic Oceanographic and Meteorological Laboratories.* Studies the physical, chemical, and geological characteristics and processes of the ocean waters, the sea floor, and the atmosphere above the ocean.

PMEL *Pacific Marine Environmental Laboratory.* Monitors and predicts the physical and biological effects of man's activities on Pacific Coast estuarine, coastal, deep-ocean, and near-shore marine environments.

GLERL *Great Lakes Environmental Research Laboratory.* Studies hydrology, waves, currents, lake levels, biological and chemical processes, and lake-air interaction in the Great Lakes and their watersheds; forecasts lake ice conditions.

GFDL *Geophysical Fluid Dynamics Laboratory.* Studies the dynamics of geophysical fluid systems (the atmosphere, the hydrosphere, and the cryosphere) through theoretical analysis and numerical simulation using powerful, high-speed digital computers.

APCL *Atmospheric Physics and Chemistry Laboratory.* Studies cloud and precipitation physics, chemical and particulate composition of the atmosphere, atmospheric electricity, and atmospheric heat transfer, with focus on developing methods of beneficial weather modification.

NSSL *National Severe Storms Laboratory.* Studies severe-storm circulation and dynamics, and develops techniques to detect and predict tornadoes, thunderstorms, and squall lines.

WPL *Wave Propagation Laboratory.* Studies the propagation of sound waves and electromagnetic waves at millimeter, infrared, and optical frequencies to develop new methods for remote measuring of the geophysical environment.

ARL *Air Resources Laboratories.* Studies the diffusion, transport, and dissipation of atmospheric pollutants; develops methods of predicting and controlling atmospheric pollution; monitors the global physical environment to detect climatic change.

AL *Aeronomy Laboratory.* Studies the physical and chemical processes of the stratosphere, ionosphere, and exosphere of the Earth and other planets, and their effect on high-altitude meteorological phenomena.

SEL *Space Environment Laboratory.* Studies solar-terrestrial physics (interplanetary, magnetospheric, and ionospheric); develops techniques for forecasting solar disturbances; provides real-time monitoring and forecasting of the space environment.

U.S. DEPARTMENT OF COMMERCE
National Oceanic and Atmospheric Administration
BOULDER, COLORADO 80302